



**Drug delivery systems based on pharmaceutically active
ionic liquids and biocompatible poly(lactic acid)**

Journal:	<i>Journal of Materials Chemistry B</i>
Manuscript ID:	TB-ART-02-2014-000264
Article Type:	Paper
Date Submitted by the Author:	17-Feb-2014
Complete List of Authors:	<p>Jouannin, claire; ICG, Chemistry Tourne-Peteilh, Corine; Institut Charles Gerhardt Montpellier - UMR 5253, MACS Darcos, Vincent; Max Mousseron institute of Biomolecules (UMR CNRS 5247), Faculty of Pharmacy - University of montpellier 1 Sharkawi, Tahmer; Institut Charles Gerhardt Montpellier - UMR 5253, MACS Devoisselle, Jean-Marie; ICG, Chemistry philippe, dieudonne; Laboratoire Charles coulomb, Gaveau, Philippe; Institut Charles Gerhardt, Solid State NMR Vioux, Andre; Laboratoire de Chimie, Universite Montpellier II Viau, Lydie; UTINAM, Chemistry</p>

Drug delivery systems based on pharmaceutically active ionic liquids and biocompatible poly(lactic acid)

*Claire Jouannin,^a Corine Tourné-Péteilh,^a Vincent Darcos,^d Tahmer Sharkawi,^a Jean-Marie Devoisselle,^a Philippe Gaveau,^a Philippe Dieudonné,^c André Vioux^a
and Lydie Viau^{a,b*}*

^a Institut Charles Gerhardt Montpellier, UMR 5253, CNRS-UM2-ENSCM-UM1 Place Eugène Bataillon, CC1701, 34095 Montpellier, France

^b Institut UTINAM, UMR CNRS 6213, UFR des Sciences et Techniques, Equipe Matériaux et Surfaces Structurés 16 route de Gray, 25030 Besançon Cedex

^c Laboratoire Charles Coulomb, UMR CNRS 5521, Université Montpellier 2, 34095 Montpellier Cedex 5, France

^d Max Mousseron Institute of Biomolecules, UMR 5247 CNRS-UM1-UM2, Faculty of Pharmacy, 15 Avenue Charles Flahault, BP 14491, 34093 Montpellier, France

* To whom correspondence should be sent: E-mail: lydie.viau@univ-fcomte.fr; Fax: + (33) 03 81 66 62 88; Tel: + (33) 03 81 66 62 93

ABSTRACT

Poly(L-lactic acid) (PLLA) membranes containing pharmaceutically active ionic liquids (API-ILs) have been prepared by simple film casting from solvent evaporation method. Several sets of membranes were prepared from two different ionic liquids namely 1-methyl-3-butyl-imidazolium ibuprofenate ($C_4MImIbu$) and lidocainium ibuprofenate ($LidIbu$) with different API-ILs contents. Scanning Electron Microscopy (SEM), Differential Scanning Calorimetry (DSC), Wide-Angle and Small-Angle X-Ray Scattering (WAXS and SAXS) revealed a strong influence of both the IL nature and its content on the morphology and the crystallinity of the resulting PLLA. At 20 weight %, $LidIbu$ was shown to act as plasticizer for PLLA and homogeneous membranes were obtained. On the contrary, at the same IL content, phase separation occurred using $C_4MImIbu$ resulting in the formation of porous PLLA. An increase of $LidIbu$ content to 50 weight % results also in phase separation. 1H and 1H - ^{13}C CP-MAS NMR measurements evidenced the influence of the different morphologies and crystallinities on IL mobility. $C_4MImIbu$ was found to be highly mobile whereas the mobility of $LidIbu$ was content dependent. At low percent, low mobility was observed while at higher content, two populations with respectively high and low mobility were observed. These PLLA-IL membranes were further tested as drug delivery system. In accordance with the morphology and mobility obtained, we demonstrated that release kinetics from PLLA membrane can be tuned by the nature and the content of API-ILs. Sustainable release kinetics were obtained with the API-IL acting as plasticizer while fastest release was obtained with the API-IL acting as porogen agent.

1. INTRODUCTION

Several issues have been related to the solid form of drugs. Polymorphism, metastability and poor aqueous solubility are the main problems that can impact their bioavailability.¹ The development of salts of the active component is one of the strategies to overcome these issues. Since 2007, there has been a growing interest in the design of room temperature Ionic Liquids (RTILs), containing active pharmaceutical ingredients (API-ILs).²⁻⁶ Other interests of ILs in the pharmaceutical field include the use of ILs or mixtures of ILs as (1) solvents for poorly soluble drugs⁷⁻¹⁰ (2) drug delivery systems in the form of microemulsions¹¹⁻¹³ and micelles.¹⁴ We reported a few years ago, the immobilization of an API-IL containing ibuprofenate anion into silica based ionogels using sol-gel process. These ionogels showed a release over hours controlled by the hydrophobicity of silica walls.¹⁵ Later on, Rogers and collaborators used the Supported Ionic Liquid Phase concept for the immobilization of API-ILs by adsorption to silica.¹⁶ The release obtained was dependent on the nature of the IL with characteristic times in the minute range.

Immobilization of ILs into polymers has been described as a way to obtain free standing membranes combining both the mechanical properties of the polymer and the ionic conductivity of the IL especially for electrochemical applications.^{17, 18} The use of polymer-IL for pharmaceutical applications is scarcer. Different ILs especially those containing phosphonium cations have been incorporated into poly(vinyl chloride) to study their plasticizing and antimicrobial activities.^{19, 20} del Monte *et al.* recently described an elegant approach to prepare poly(diol-*co*-citrate) elastomers loaded with lidocaine by using deep eutectic solvents (DES) based on mixtures of 1,8-octanediol and lidocaine. The originality of the method is based on the use of DES which provide the polymer, the API and the synthetic media where the second polymer precursor is solubilized.²¹ More recently, two biocompatible choline-based ILs were

incorporated into a polyelectrolyte (chitosan) to study their effect on the conductivity of the chitosan films and their influence on the release profile of an ionic drug, sodium phosphate dexamethasone. In this case, it has been demonstrated that release was not controlled by diffusion or swelling but mainly influence by ionic interactions between the components (IL/drug/polyelectrolyte).²²

In this article, we describe the preparation of poly(L-lactic acid) (PLLA) membranes incorporating API-ILs. PLLA is a biodegradable and biocompatible polymer that has already been used in various biomedical applications such as surgical sutures, bone fixation devices and drug-delivery systems.^{23, 24} ILs, especially those containing imidazolium cations, have been described as plasticisers for PLA.²⁵ Very recently, Kim and collaborators described the formation of microporous PLLA by a phase-separation method using imidazolium ionic liquids as the porogen.²⁶ The efficiency of the micropore network in loading and releasing drugs and proteins was also investigated.²⁷

We used two ILs comprising the same ibuprofenate anion. We chose to study 1-methyl-3-butyl-imidazolium ibuprofenate, C₄MImIbu, to compare our results with those we obtained using silica.¹⁵ The second IL investigated is lidocainium ibuprofenate,¹⁶ LidIbu, that is a protic ionic liquid presenting weak ionicity. Actually, some protic API-ILs have been shown to form hydrogen bond clusters and to diffuse faster through membranes.²⁸ This IL has also previously been incorporated into silica matrices for drug delivery application.¹⁶

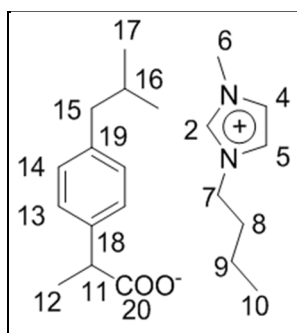
This study demonstrates the influence of the API-IL nature and content on PLLA morphology, crystallinity and thermal stability and shows that these parameters could be related to drug release kinetics. Several techniques were used to investigate the morphology and the crystallinity of the PLLA-IL membranes, such as Scanning Electron Microscopy (SEM), differential scanning calorimetry (DSC), wide-angle and small-angle X-Ray diffraction (WAXS and SAXS). Solid

state NMR was also performed to study the IL mobility inside the membrane. Finally, *in vitro* drug release kinetics were measured in simulated physiological media at 37°C to evaluate the potential of these membranes to act as drug delivery systems.

2. EXPERIMENTAL SECTION

Chemicals. The following chemicals were purchased and used as received: 4-Isobutyl- α -methylphenylacetic acid 99 % (ibuprofenic acid) from Alfa Aesar, 1-butyl-3-methylimidazolium hydrogen carbonate solution $C_4MimHCO_3$ (50 wt% in Methanol/H₂O 2:3), lidocaïne, potassium phosphate monobasic and sodium hydroxide from Sigma-Aldrich, and chloroform from VWR.

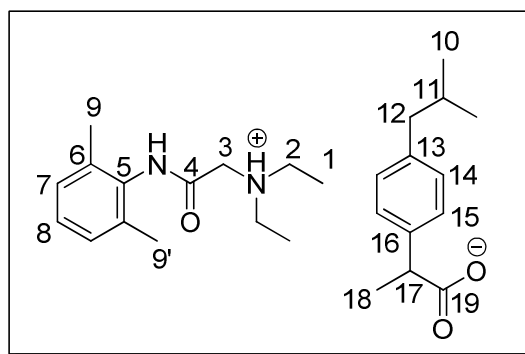
Synthesis of 1-methyl-3-butylimidazolium ibuprofenate $C_4MimIbu$



Ibuprofen (1.00 g, 4.88 mmol) was dissolved into 10 mL of absolute ethanol. $C_4MimHCO_3$ (1.95 g, 4.89 mmol) was dissolved into 2 mL of ethanol and added slowly to the previous solution. The resulting mixture was stirred at room temperature for 4 hours. The solvent was removed under vacuum at room temperature and further dried at 70 °C under vacuum overnight. The final product was obtained as a pale yellow very viscous liquid (1.57 g, 94 %). 1H NMR (200 MHz, $CDCl_3$) : δ = 11.39 (s, 1H, H₂) ; 7.27 (d, J = 7.9 Hz, 2H, H₅, H₄) ; 6.91 (d, J = 7.9 Hz, 4H, H₁₄, H₁₃) ; 4.11 (t, J = 7.3 Hz, 2H, H₇) ; 3.81 (s, 3H, H₆) ; 3.56 (q, J = 7.2 Hz, 1H, H₁₁) ; 2.32 (d, J =

7.1 Hz, 2H, H₁₅) ; 1.69 (m, 3H, H₈, H₁₆) ; 1.42 (d, $J = 7.1$ Hz, 3H, H₁₂) ; 1.22 (m, 2H, H₉) ; 0.85 (m, 9H, H₁₀, H₁₇). ¹³C NMR (75.5 MHz, CDCl₃) : $\delta = 179.3$ (C₂₀); 141.8 (C₁₈/C₁₉); 139.9 (C₂); 137.2 (C₁₈/C₁₉); 127.4 (C₁₃/C₁₄); 126.2; (C₁₃/C₁₄) 121.2 (C₄/C₅); 119.5 (C₄/C₅); 48.3 (C₇); 48.2 (C₁₁); 43.9 (C₁₅); 34.9 (C₆); 30.9 (C₈); 29.1 (C₁₆); 21.3 (C₁₇); 18.6 (C₁₂); 18.3 (C₉); 12.3 (C₁₀). m/z (ES⁺) 139 (M⁺, 100). m/z (ES⁻) : 205 (M⁻, 100) , 411 (2M⁻+H⁺]. $\nu_{\max}/\text{cm}^{-1}$ 3138 and 3045 (ν C=C-H imidazolium and phenyl rings), 2954, 2927, 2867 (ν C-H alkyls), 1581 and 1373 (ν COO⁻). TGA : T_{d 5%} = 217 °C, T_g = -33 °C. Water content \leq 200 ppm.

Synthesis of lidocanium ibuprofenate LidIbu



Ibuprofenic acid (1.00 g, 4.85 mmol) and lidocaine free base (1.14 g, 4.85 mmol) were melted with stirring until a free-flowing clear liquid was obtained.¹⁶ The mixture was cooled to room temperature to obtain the product as a pale yellow liquid. ¹H NMR (600 MHz, CDCl₃) δ (ppm) = 9.04 (s, 1H, H_{NH}), 7.21 (dd, $J = 8.1$ Hz, 2.2 Hz, 2H, H₁₅), 7.12 - 7.03 (m, 5H, H₇/H₈/H₁₄), 3.75 - 3.66 (m, 1H, H₁₇), 3.31 (s, 2H, H₃), 2.79 - 2.72 (m, 4H, H₂), 2.44 (d, $J = 7.1$ Hz, 2H, H₁₂), 2.24 (s, 3H, H₉), 2.23 (s, 3H, H₉), 1.84 (m, 1H, H₁₁), 1.50 (m, 3H, H₁₈), 1.17 (m, 6H, H₁), 0.90 (d, $J = 6.6$ Hz, 6H, H₁₀). ¹³C NMR (151 MHz, CDCl₃) δ (ppm) = 179.7 (C₁₉), 169.3 (C₄), 140.4 (C₁₃), 138.2 (C₁₆), 135.2 (C₆), 133.8 (C₅), 129.3 (C₁₄), 128.3 (C₇), 127.3 (C₈/C₁₅), 56.6 (C₃), 48.7 (C₂), 45.6 (C₁₂), 45.1 (C₁₇), 30.2 (C₁₁), 22.5 (C₁₀), 18.5 (C₉/C₁₈), 11.9 (C₁). $\nu_{\max}/\text{cm}^{-1}$: 3226 (ν C=C-H

phenylrings), 2953, 2923, 2869 (ν C-H alkyls), 1686 (ν C=O), 1499, 1458, 1383 (ν COO⁻), 1089, 1068, 767. TGA : $T_{d5\%} = 223$ °C. DSC : $T_g = -26$ °C. Water content ≤ 100 ppm.

Synthesis of poly(L-lactic acid)

Poly(L-lactic acid) (PLLA) was synthesised by ring opening polymerisation of L-lactide using zinc lactate as the catalyst. Briefly the solid monomer feed was introduced in a glass flask together with 0.05 % w/w of powdered zinc lactate (Aldrich, France). The flask was connected to a dynamic vacuum line and the feed was melted under vacuum. Several vacuum/dry nitrogen cycles were performed to eliminate oxygen and water traces from the feed. The flask was finally sealed under vacuum. The monomer feed was allowed to polymerize for 15 days at 145 °C. At the end, the flask was opened and the polymeric mass dissolved in dichloromethane. The polymer was precipitated using ethanol and finally dried under vacuum. Purified polymer yield was 65-70 % of monomer feed. ¹H NMR (300 MHz, CDCl₃) : $\delta = 5.10$ (q, $J = 6.9$ Hz, 1H) ; 1.44 (d, $J = 6.9$ Hz, 3H). ¹³C NMR (75.5 MHz, CDCl₃) : $\delta = 168.6$; 68.0; 15.6. $\nu_{\max}/\text{cm}^{-1}$: 2998 and 2947 (CH-CH₃), 1747 (C=O), 1455, 1383, 1359 (CH₃), 1205, 1180, 1129, 1084, 1043 (-C-C-O), 871 (C-COO), 755 and 686 (C=O). SEC (chloroform): M_n 120 000 g.mol⁻¹; $D = 1.27$. TGA : $T_{d5\%} = 334$ °C. DSC : $T_g = 61$ °C, $T_c = 82$ °C, $T_m = 173$ °C.

Synthesis of PLLA-IL membranes

PLLA-IL membranes were prepared by the solvent-casting method. PLLA (typically 50 mg) was dissolved in CHCl₃ at a concentration of 25 g/L. The ionic liquids LidIbu and C₄MImIbu were dissolved in CHCl₃ at different concentrations, from 20 weight % to 100 weight % relative to the PLLA. PLLA and IL in chloroform were then mixed together and poured onto a Teflon support. After slow evaporation of the solvent at room temperature, the membranes were further dried under vacuum overnight at 60°C. PLLA membranes (without IL) were similarly prepared by

dissolution of PLLA in CHCl_3 , poured onto a Teflon support, followed by slow evaporation of the solvent at room temperature for 3 days and complete drying under vacuum overnight at 60°C . Samples obtained using a mixture of PLLA and LidIbu or C_4MImIbu are named PLLA-LidIbu_x and PLLA- $\text{C}_4\text{MImIbu}_x$, respectively, where x represents the weight percent of IL relative to PLLA. The membranes were stored under inert atmosphere and used within 5 days for drug release experiments.

Characterizations. **Thermogravimetric analysis (TGA)** were carried out on a Netzsch STA 409 PC Luxx in alumina crucible under an air flow with a heating rate of $5^\circ\text{C}/\text{min}$ up to 850°C followed by an isotherm at 850°C for 30 min. **Differential Scanning Calorimetry (DSC)** Measurements of phase-transition temperatures were performed with a Netzsch differential scanning calorimeter model 204F1 Phoenix and the data were evaluated using Netzsch Proteus Thermal Analysis software version 4.8.1. Samples of 5-10 mg were placed in a hermetically sealed aluminum pan; an empty pan was used as reference. Pans were exposed to a N_2 flow atmosphere. The following conditions measurements were applied: 1) cooling from room temperature to -70°C at a rate of $10^\circ\text{C}/\text{min}$ 2) isotherm at -70°C for 5 min 3) heating to 200°C at a rate of $10^\circ\text{C}/\text{min}$. The glass transition temperature T_g was determined at the midpoint of a heat-capacity change. The melting temperature T_m was taken at the onset of the melting endotherm. Calibration was performed with indium, zinc, bismuth and cesium chloride. The degree of crystallinity χ_c was calculated from the following equation:

$$\chi_c = \frac{\Delta H_m + \Delta H_c}{\Delta H_m^0} \times 100$$

where ΔH_m^0 is the heat of fusion for the perfectly crystalline PLLA (93 J/g),²⁹ ΔH_m and ΔH_c are the enthalpies of fusion and crystallization respectively in J/g of PLLA.

Size Exclusion Chromatography (SEC) of PLLA was performed with a system equipped with a guard column (50 × 7.5 mm) followed by a PL gel 5 μm Mixed C column (300 × 7.5 mm). Chloroform was used as eluent at a flow rate of 0.5 mL/min (Shimadzu LC 20AD pump). The measurements were carried out at 22 °C with a polymer sample concentration of 5 mg/mL. Samples previously used in simulated intestinal media were washed with water and ethanol prior to SEC analysis in order to remove remaining salts. Before the injection (50 μL), the samples were filtered through a PTFE membrane with a 0.45 μm pore. After column exclusion, the samples were analyzed with a RI Shimadzu RID 10A refractometer, a Waters 486 UV detector and a Wyatt TREOS light diffusion detector. SEC system was calibrated with polystyrene standard. Data processing was carried out with WTC ASTRA software from Wyatt. **Contact angle measurements** were performed with a Digidrop Fast 60 contact angle meter (GBX, France) using 2 μL drops of Millipore water. Contact angle measurements were repeated at least 4 times for each sample and were analyzed with Windrop+ v4.11c software. **Water content** was determined with a Schott Titroline KF Karl Fischer titrator. **¹H and ¹³C liquid-state NMR** were recorded on Bruker AVANCE DPX 200, AVANCE 300 and AVANCE III 600 spectrometers at room temperature. Chemical shifts (δ) are given in ppm and are referenced to residual solvent peaks (CDCl₃: δ 7.26 ppm ¹H; δ 77.0 ppm ¹³C). Coupling constants (*J*) are reported in Hz. **¹H and ¹³C solid-state NMR** were performed on a Varian VNMRs600 Wide Bore spectrometer (14.09 T) using a 3.2 mm MAS probe. Samples were packed as tightly rolled membranes in ZrO₂ rotors spun at 10 kHz. ¹H spectra were acquired using a π/2 single pulse of 2.5 μs with a 10 s recycling delay. ¹H-¹³C CP-MAS spectra were acquired using a ramped 2 ms contact time with proton decoupling and a 5 s recycling delay. ¹H and ¹³C chemical shifts were reference using adamantane as a secondary reference. **Scanning Electron Micrographs.** A HITACHI S4800

Scanning Electron Microscope (SEM) was used to examine the cross section of the membranes. SEM samples were cryo-fractured in liquid nitrogen. **Polarized Optical Microscopy (POM)** observations were performed on a Carl Zeiss Aviolab polarized optical microscope equipped with a digital camera. **Membranes thicknesses** were measured using a digital micrometer. Thicknesses were measured in at least 3 different points for each membrane. **Small Angle X-Ray Scattering (SAXS) and Wide Angle X-Ray Scattering (WAXS)** experiments were performed with an in-house setup of the *Laboratoire Charles Coulomb, "Réseau X et gamma", Université Montpellier 2, France*. A high brightness low power X-ray tube, coupled with a spheric multilayer optic (GeniX^{3D} from Xenocs) was employed. It delivers an ultralow divergent beam (0.5 mrad). Scatterless slits were used to give a clean 0.8 mm beam diameter (35 Mphotons/s) at the sample. We worked in a transmission configuration and scattered intensity was measured by a Schneider 2D image plate detector prototype, at a distance of 1.9 m from the sample for SAXS configuration, 0.2 m from the sample for WAXS configuration. All Intensities were corrected by transmission and the empty cell contribution was subtracted.

***In vitro* release tests** *In vitro* release tests were performed (in triplicate) in a standard pharmaceutical dissolutest USP1 apparatus. 1 L vessels were filled with 0.3 L of phosphate simulated medium (NF18/USP 23: 13.6 g of KH₂PO₄ in 2.0 L of distilled water, adjusted to pH 7.4 with NaOH 1N). The temperature was set at 37 °C, and the paddle speed at 80 rpm. The membranes were cut into rectangular shape samples of 6 cm × 1.5 cm previously to immersion. Samples of 1 mL were taken for HPLC analysis and replaced by fresh medium. Ibuprofen releases were quantified by HPLC (LC-2010 AHT, Shimadzu) on a C18 Prontosil 120 Å, 5 µm (250x4.6 mm) column, the mobile phase was CH₃CN / 0.5 % acetic acid (65 : 35), with a flow rate of 1.2 mL/min, UV detector wavelength was set at 230 nm. Lidocaine releases were

quantified by HPLC (LC-2010 AHT, Shimadzu) on a C18 Prontosil 120 Å, 5 µm (250x4.6 mm) column, the mobile phase was CH₃CN / KH₂PO₄ at 4.85 g/L pH 8.0 (70 : 30), with a flow rate of 1.2 mL/min, the UV detector wavelength was set at 230 nm. C₄MIm releases were quantified by HPLC (LC-2010 AHT, Shimadzu) on a C18 Prontosil 120 Å, 5 µm (250x4.6 mm) column, the mobile phase was CH₃CN/KH₂PO₄ at 4.85 g/L pH 8.0 (40 : 60), with a flow rate of 1.2 mL/min, the UV detector wavelength was set at 210 nm.

3. RESULTS AND DISCUSSION

ILs and membranes synthesis

The chemical structures of the investigated ILs and PLLA are shown in Figure 1. We improved and simplified our previous method¹⁵ to synthesize C₄MImIbu: 1-butyl-3-methylimidazolium hydrogen carbonate solution was reacted with a stoichiometric amount of Ibuprofen at room temperature. This method is more efficient as carbon dioxide and water are the only by-products. LidIbu was synthesized according to a published method *i.e* by acid base reaction between ibuprofen and lidocain.¹⁶ The resulting ILs were carefully dried overnight at 70°C under reduced pressure before use. High molecular weight PLLA was synthesized in bulk by ring opening polymerisation of L-lactide using zinc lactate as the catalyst ($M_n = 120,000 \text{ g.mol}^{-1}$, $D = 1.27$). PLLA-ILs membranes were prepared by film casting from solvent evaporation method. The detailed experimental procedures are given in the experimental section. Formulations of different weight percent of ILs were investigated. Solid membranes were obtained in all cases for LidIbu in the composition range studied (from 20 weight % to 100 weight % relative to the PLLA). However, at 75 weight % of C₄MImIbu, drops of IL were clearly visible on the surface of the membrane. Here, we only reported results obtained with 20 weight % (PLLA-LidIbu₂₀), 50 weight % of LidIbu (PLLA-LidIbu₅₀) and 20 weight % of C₄MImIbu (PLLA-C₄MImIbu₂₀). These results are indeed the more interesting to demonstrate the influence of the IL nature and IL content on PLLA crystallinity and morphology and drug release kinetics. The obtained PLLA-IL membranes have a thickness of ca. $42 \mu\text{m} \pm 1 \mu\text{m}$. It should be noted that in the same conditions, pure ibuprofen or lidocaine could not be immobilized into PLLA membranes.

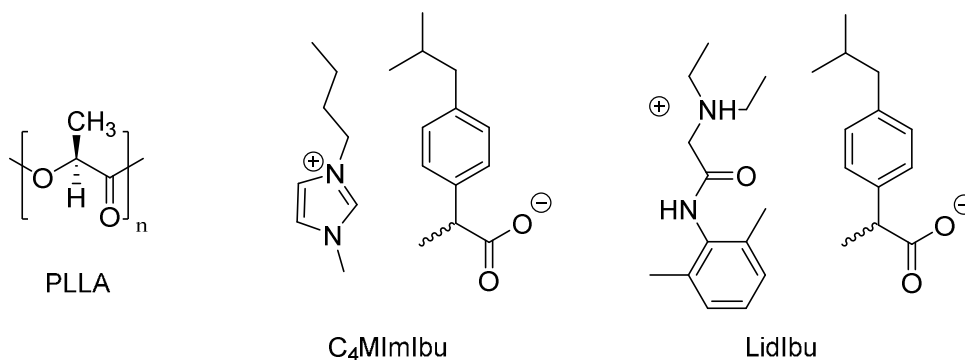


Figure 1. Structures of PLLA and IL investigated.

Effect of API-ILs on PLLA morphology

To address this point, the cross-sections of PLLA and PLLA-IL membranes were evaluated by SEM (Figure 2). The samples were analyzed after careful removal of the IL by washing the membranes several times with ethanol. The PLLA membrane was submitted to the same treatment for comparison. The cross-sectional images of the PLLA membrane demonstrate the formation of a dense film. As shown in Figure 2b, the PLLA-LidIbu₂₀ is also very dense, indicating that the blend forms a homogeneous mixture. On the contrary, PLLA-LidIbu₅₀ (Figure 2c) and PLLA-C₄MImIbu₂₀ (Figure 2d) membranes show a sponge-like structure characteristic of phase separation with pores of about 1.5 μm. The porous structure is homogeneously distributed into the polymer.

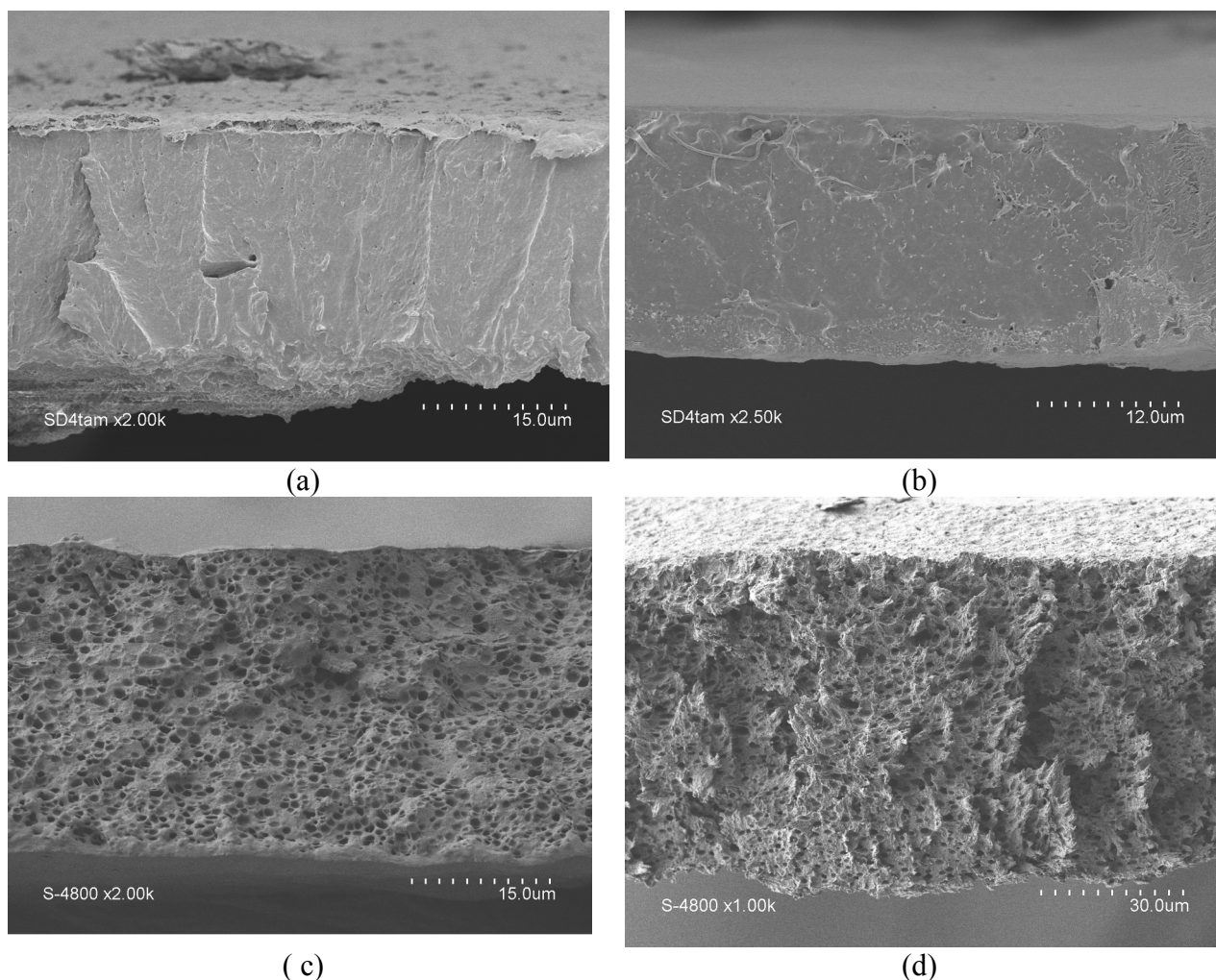


Figure 2. SEM of membranes cross-section (a) PLLA (b) PLLA-LidIbu₂₀ (c) PLLA-LidIbu₅₀ and PLLA-C₄MimIbu₂₀ (d) after removal of the IL.

We then investigated the compatibility of the two different ILs with PLLA by means of DSC. DSC thermograms of PLLA, PLLA-IL membranes and pure ILs are shown in Figure 3 and the corresponding data are summarized in Table 1. As expected for a semi-crystalline polymer, PLLA presents in the first heating scan, a glass transition at 61°C as well as a crystallization exotherm at 82 °C and a melting endotherm peak at 173°C. The ILs LidIbu and C₄MimIbu show only a glass transition T_g at respectively -26°C and -33°C. The DSC thermogram of the PLLA-LidIbu₂₀ sample presents a broad glass transition at around 30°C and a melting peak at lower

temperature than for pure PLLA. The observation of a single T_g at temperature in-between those of PLLA and LidIbu confirms that the two components are miscible in this proportion and that LidIbu acts as plasticizer of PLLA. Partial miscibility between PLLA and hyperbranched poly(ester amide) HBP have been also observed by Lin and collaborators. They gave evidences by FTIR analysis of H-bonding involving the C=O function of PLLA with NH functions of HBP.³⁰ In our case, no evidence of such hydrogen bonding was found by FTIR (results not shown).

Upon increasing LidIbu content to 50 w% (PLLA-LidIbu₅₀), two T_g s are distinguishable: the first at 35°C close to the T_g of the single phase PLLA-LidIbu₂₀ and a second one at -24°C close to the value of LidIbu (- 26°C). The presence of two T_g s is in accordance with the phase separation observed by SEM. However, one part of LidIbu is partially miscible with PLLA. In the case of total phase separation two glass transitions would have been observed: one at the glass transition of PLLA (62 °C) and one for the glass transition of LidIbu (-26 °C). The LidIbu₅₀ membrane is indeed constituted of two phases, one with a composition close to the PLLA-LidIbu₂₀ membrane and a second one consisting of LidIbu which percolates through the PLLA network. Interestingly, no cold crystallization peaks were detected for PLLA-LidIbu membranes showing that a large amount of PLLA had already crystallized. This behavior can be explained as follows: when the amount of LidIbu, which acts as a plasticizer, is increased, PLLA chains have enough mobility to rearrange and crystallization is favored. The amorphous domain in PLLA, and consequently the amount of plasticizer, is reduced and phase separation occurs.³¹ The enhancement of the crystallinity is clearly visible from the increase of the degree of crystallinity χ_c in the case of PLLA-LidIbu₂₀ membrane (Table 1).

The DSC trace of PLLA-C₄MImIbu₂₀ is similar to that of PLLA. From SEM measurements, it was evidenced that phase separation occurred also in this case thus, two T_g s should have been observed. We assumed that the C₄MImIbu content was too low to be detected.

Finally, it is worth pointing out that a small exothermal peak just prior to the melting was observed for PLLA and PLLA-C₄MImIbu₂₀ membranes. This peak has been ascribed to a disorder to order (α' to α) solid-solid phase transition.^{32, 33} The α' form first described by Zhang *et al* is obtained when PLLA is crystallized below 100 °C, while the α form is developed above 120 °C.³⁴ The absence of this peak for PLLA-LidIbu membranes and the absence of cold-crystallisation peak suggest the formation of a stable crystalline phase.

Kim and collaborators have recently obtained porous PLLA scaffold by phase separation using imidazolium ionic liquids as porogen. They demonstrated that porous scaffold could only be obtained using hydrophilic ionic liquids²⁷. Our results are consistent with them as C₄MImIbu can be consider as hydrophilic while the protic LidIbu which presents low ionicity is more hydrophobic. Moreover, the same authors removed the IL porogen from the PLLA and then loaded different drugs and proteins to study the drug release behavior of the porous PLLA scaffold. Here, we show that macroporous PLLA membranes incorporating API can be prepared in a single step.

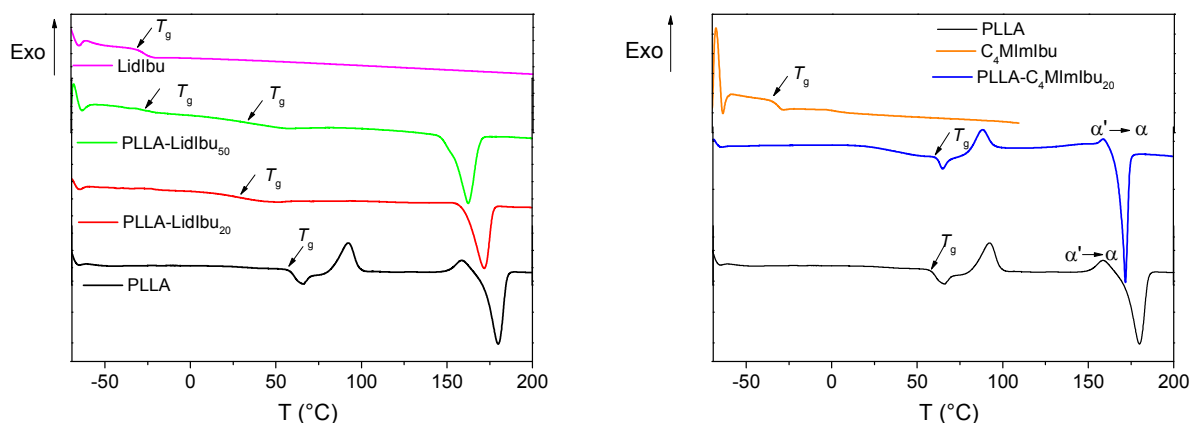


Figure 3. DSC heating scans of PLLA, PLLA-LidIbu (left) and PLLA-C₄MimIbu membranes (right) from -70°C to 200°C at a heating rate of 10°C/min.

Table 1. Thermal properties of the ILs and the PLLA-IL membranes

Sample	T_g (°C)	T_c (°C)	ΔH_c^a (J/g)	T_m (°C)	ΔH_m^a (J/g)	χ_c (%)
PLLA	61	82	-15	173	30	16
LidIbu	-26					
PLLA-LidIbu ₂₀	26			161	25	27
PLLA-LidIbu ₅₀	-24 and 35			156	17	18
C ₄ MimIbu	-33					
PLLA-C ₄ MimIbu ₂₀	63	80	-9	169	32	23

^a per gram of PLLA

Effect of API-ILs on PLLA crystallinity

DSC measurements have suggested a higher crystallinity in the case of PLLA-LidIbu membranes. To confirm these assumptions, we performed WAXS analysis (Figure 4). For clarity reasons, the profiles of the weak reflections are enlarged in panel b of figure 4 and all the diffraction patterns have been normalized using the strongest 200/100 reflection intensity (see below). The semi-crystalline PLLA membrane presents a broad amorphous halo between 8° and 25° 2θ and two well resolved crystalline peaks at $2\theta = 16.4^\circ$ and $2\theta = 18.7^\circ$ assigned respectively

to diffractions from the (110/200) and (203) planes. Moreover, from the values of these diffraction peaks it can be concluded that PLLA is in a α' crystalline form.³⁵ The WAXS pattern does not undergo much of changes upon incorporation of C₄MImIbu whereas the PLLA-LidIbu membranes present higher crystallinity as evidenced by the decrease of the amorphous halo intensity. Moreover, the (110)/(200) and (203) reflections shift to higher 2θ values and new diffraction peaks at $2\theta = 12.5$ (004/103), $2\theta = 14.7$ (010), $2\theta = 20.7$ (204), $2\theta = 22.3$ (015), $2\theta = 23.8$ (016) and $2\theta = 27.3$ (207) are observed. This WAXS pattern is characteristic of the more stable crystalline α -form of PLLA.³⁵

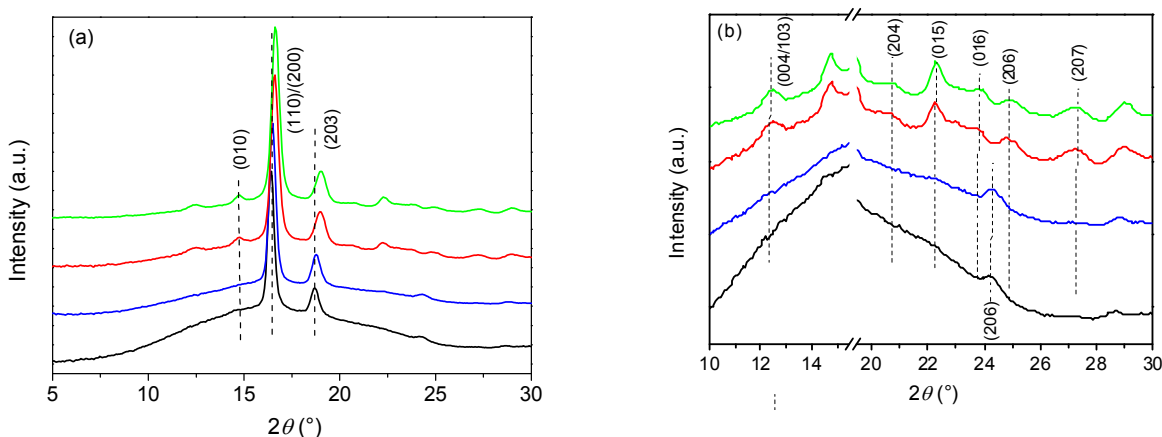


Figure 4. (a) WAXS patterns and (b) enlarged patterns of (-) PLLA, (-) PLLA-C₄MImIbu₂₀, (-) PLLA-LidIbu₂₀ and (-) PLLA-LidIbu₅₀.

Figure 5 shows the Lorentz corrected SAXS profile $I(q)q^2$ v.s. q where $q = 4\pi \sin\theta/\lambda$ (θ = scattering angle, λ = wavelength) of PLLA and PLLA-IL membranes. One scattering peak characteristic of a lamellar structure is observed at $q^* = 0.296 \text{ nm}^{-1}$ for PLLA-LidIbu₂₀. The peak position shifted gradually to larger scattering vectors ($q^* = 0.307 \text{ nm}^{-1}$) with increasing the LidIbu content (PLLA-LidIbu₅₀).

The long periods (L) were calculated with the Bragg equation:

$$L = \frac{2\pi}{q^*}$$

q^* being the scattering vector of maximum intensity of the Lorentz-corrected SAXS curves. They are equal to 21.2 nm and 20.5 nm respectively for PLLA-LidIbu₂₀ and PLLA-LidIbu₅₀.³⁶ No characteristic peak was observed for PLLA and PLLA-C₄MImIbu indicating the absence of periodic structure. In accordance with WAXS and SAXS results, the polarized optical micrographs of PLLA-LidIbu membranes obtained at 25 °C present spherulites showing the familiar Maltese cross birefringence characteristic of lamellar structures (Figure S1).

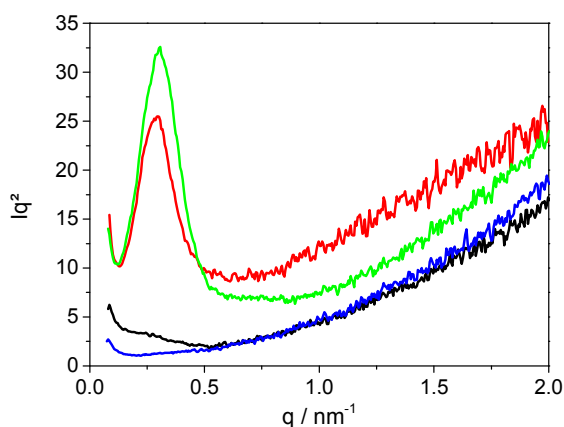


Figure 5. Lorentz corrected SAXS patterns of (-) PLLA, (-) PLLA-C₄MImIbu₂₀, (-) PLLA-LidIbu₂₀ and (-) PLLA-LidIbu₅₀

API-ILs mobility into the PLLA membrane

We then investigated the molecular mobility of the different ILs into the PLLA membranes by solid state NMR. We first conducted ¹H MAS NMR experiments as line widths are very sensitive to molecular motion. Indeed, rotational molecular motion can effectively reduce the proton–proton nuclear spin dipolar couplings that dominate the ¹H MAS NMR line shape. As a result, a

decrease in the line width is indicative of increased molecular motion. Figure 6a compares the solid state ^1H MAS NMR spectra of PLLA and PLLA-IL membranes recorded at a spinning rate of 10 KHz with the liquid state ^1H NMR spectrum of LidIbu and C_4MImIbu . The ^1H MAS NMR spectrum of PLLA presents two broad bands centred at 5.8 ppm (δ CH_2) and 1.8 ppm (δ CH_3) characteristic of a rigid lattice. The spectrum of the PLLA-LidIbu₂₀ membrane also presents the same two broad bands attributed to PLLA. However, no signal characteristic of LidIbu was observed indicating a complete molecular dispersion of the IL into PLLA. When increasing the LidIbu content (PLLA-LidIbu₅₀) the spectrum changes dramatically, narrower signals attributed to the IL are detected while the signals of PLLA are hardly observable. Also, in the PLLA- $\text{C}_4\text{MImIbu}_{20}$ membranes the signals characteristic of C_4MImIbu are predominantly observed and these signals are much narrower than in the case of PLLA-LidIbu. Such narrowing of the signals provides direct evidences of higher molecular mobility.

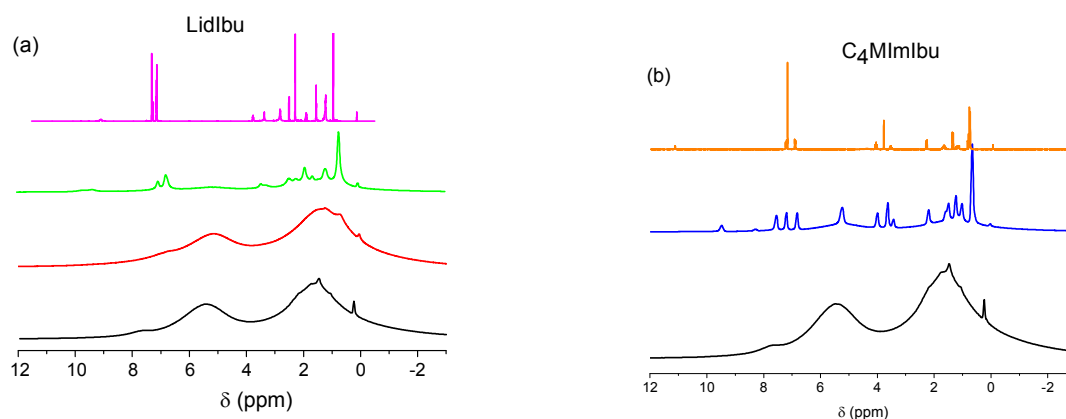


Figure 6 . (a) ^1H MAS NMR spectra of (-) PLLA, (-) PLLA-LidIbu₂₀, (-) PLLA-LidIbu₅₀ and (-) ^1H NMR of LidIbu in CDCl_3 (b) ^1H MAS NMR spectra of (-) PLLA, (-) PLLA- $\text{C}_4\text{MImIbu}_{20}$ and ^1H NMR of C_4MImIbu in CDCl_3 .

We then performed ^1H - ^{13}C CP-MAS NMR to selectively detect the rigid components in the membranes (Figure 7). As can be seen in Figure 7a three well-resolved peaks characteristic of

PLLA are observed at 170.3 ppm (carbonyl), 69.6 ppm (methine) and 17.1 ppm (methyl). However, a closer inspection of the spectrum (Figure 7b) reveals the existence of additional smaller peaks in the case of PLLA-LidIbu₂₀ and PLLA-LidIbu₅₀ membranes corresponding to the rigid carbon atoms of LidIbu (signals pointed by the arrows). In the same conditions, no signal characteristic of the carbon of C₄MImIbu was observed.

Thus, these two different NMR experiments (¹H and ¹H -¹³C CP-MAS) demonstrate that C₄MImIbu has a high mobility in the membranes whereas LidIbu is more constrained. However, a strong difference exists depending on the LidIbu content. In the PLLA-LidIbu₂₀ membrane, the IL is poorly mobile, whereas in the case of PLLA-LidIbu₅₀, two components are clearly visible, one with a high mobility and another one more rigid. These results are in accordance with the fact that two *T_g*s have been observed by DSC, one close to that of pure LidIbu and one resulting from the miscibility of PLLA with LidIbu.

Figures 7c and 7d present a zoom of the carbons corresponding to the PLLA. Each carbon of PLLA and PLLA-C₄MImIbu₂₀ membranes exhibits a single and broad resonance, whereas the resonance of these carbons splits into multiple peaks for PLLA-LidIbu membranes. Such features were recently observed by Pan and collaborators.³⁷ They demonstrated that the α' form of PLLA presents broad signals in the NMR spectra, while resonances splitting are obtained for the α form. Such splitting was attributed to crystallographically inequivalent sites within the crystal unit cell. These observations are consistent with our DSC measurements (see above).

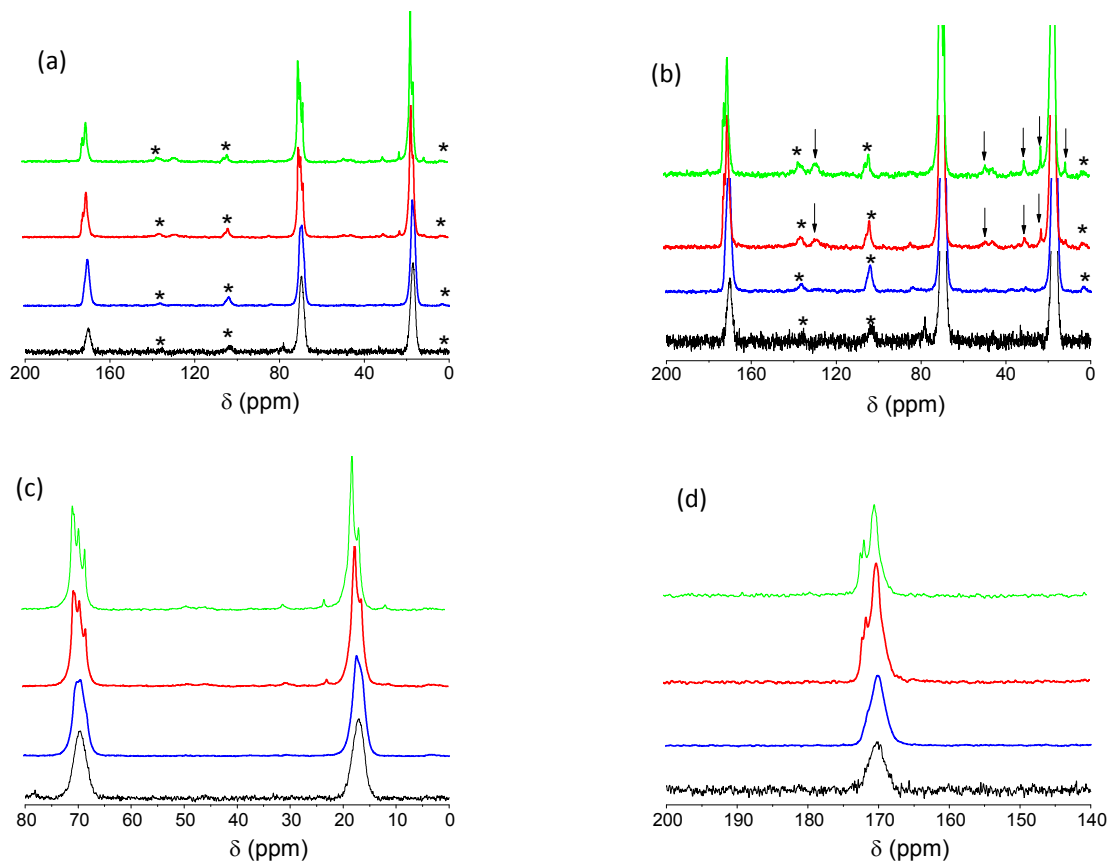


Figure 7. ^1H - ^{13}C CP-MAS NMR spectra of (-) PLLA, (-) PLLA- $\text{C}_4\text{MimIbu}_{20}$ (-) PLLA-LidIbu $_{20}$ and (-) PLLA-LidIbu $_{50}$ (a) full spectra (b) enlarged spectra (c) methylene and methyl carbon resonances (d) carbonyl resonances *spinning sidebands \rightarrow LidIbu signals

Drug release parameters

Before the release experiments, we studied the degradation of PLLA-IL membranes by TGA and SEC measurements. The thermal stabilities of the PLLA-IL membranes before release are shown in Figure S2. Clearly, both ILs promote PLLA thermal degradation and the lowest stability was obtained with C_4MimIbu . Molecular weight values determined before release experiments, (within 5 days after membranes synthesis) show that both ILs accelerate the degradation of PLLA (Table 2). The highest degradation is obtained in the presence of the highest IL content. However, for the same IL content the degradation is independent to the nature of the IL. Xanthos and collaborators reported the same effect using phosphonium ILs containing dodecanoate anions

and ascribed the acidic catalytic degradation to the presence of carboxylic group.³⁸ In our case, the presence of the carboxylate function on the ibuprofenate might as well be responsible for the polymer degradation observed.

Table 2 Molecular weight (M_p) and dispersity (\mathcal{D}) of PLLA determined by SEC in chloroform

	PLLA		PLLA/ C ₄ MImIbu ₂₀		PLLA/ LidIbu ₂₀		PLLA/ LidIbu ₅₀	
	M_p (g.mol ⁻¹)	\mathcal{D}	M_p (g.mol ⁻¹)	\mathcal{D}	M_p (g.mol ⁻¹)	\mathcal{D}	M_p (g.mol ⁻¹)	\mathcal{D}
t = 0	94,000	1.3	83,000	1.2	84,000	1.2	78,000	1.3

In vitro drug release kinetics were measured (in triplicate) in simulated media at 37°C in a standard pharmaceutical dissolution test (USP 1) under Sink conditions.³⁹ Kinetics were monitored by HPLC, based on the typical retention time of ibuprofen, lidocaine and C₄MIm respectively. Figure 8 presents release profiles obtained during 27 days and the inset shows kinetics for the first 8 hours. In all membranes investigated, the anion and the cation of the IL are released at the same time, within experimental errors. Release kinetics agreed well with the morphology and the IL mobility. The fastest drug release was obtained with the PLLA-C₄MImIbu₂₀ membranes showing higher phase separation and higher ionic liquid mobility. A burst effect was observed with 50% release in 1 minute and a maximum amount of drug release of 70% after two hours. The PLLA-LidIbu₅₀ membranes present a fast release with 40% release in few minutes and slower release with 90% release within 2 hours. As expected from its higher compatibility and lower mobility, LidIbu in the PLLA-LidIbu₂₀ membrane exhibited sustained release occurring within 16 days. In this latter case, closer inspection of the kinetics provides evidence of two regimes. The first one occurs within 8 hours and is controlled by diffusion. After that, zero-order kinetics are observed that could be due to a combination of drug diffusion and

PLLA degradation.⁴⁰

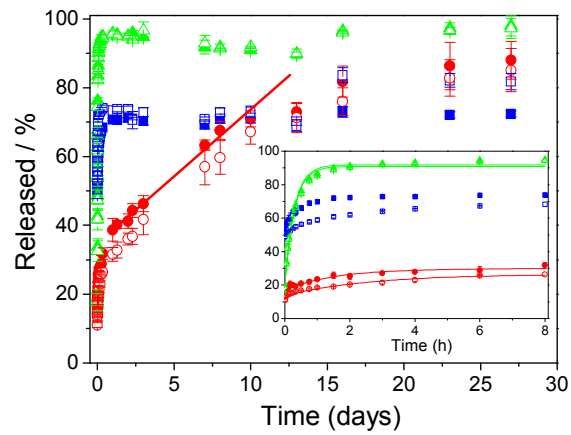


Figure 8. Release kinetics obtained for PLLA-C₄MImIbu₂₀ , PLLA-LidIbu₂₀ and PLLA-LidIbu₅₀. Close symbols: Ibu, open symbols: C₄MIm or Lid.

4. CONCLUSION.

In conclusion, API-ILs have been incorporated for the first time into PLLA membranes. The miscibility of the IL with PLLA was demonstrated to be dependent on the IL content and its nature. In the case of C₄MImIbu, phase separation occurs even at low IL content resulting in the formation of a porous PLLA membrane. Incorporation of drugs into porous PLLA membranes is usually performed into two steps consisting in the formation of the porous membrane followed by drug loading. Here, we synthesized in a single step a porous membrane containing the drug using the IL both as porogen and API. Incorporation of the IL into the polymer voids results in very fast release kinetics of the API-IL. The case of LidIbu is interesting, as at low content it is totally miscible with PLLA and acts as a plasticizer while at higher content phase separation is observed. Moreover, WAXS, DSC and solid state NMR analysis have evidenced the formation of a stable α PLLA crystalline phase using LidIbu. Interestingly, this phase was obtained at room temperature while crystallization temperatures higher than 120°C are usually necessary. In accordance with morphology results, drug release kinetics can be modulated by an appropriate choice of the IL. Using the same ibuprofenate anion, we have shown that sustained release occurred within 27 days using lidocainium cation, while faster release (few hours) was obtained with imidazolium cation. However, there is a limitation of the investigation of ILs which possess carboxylate function responsible for PLLA degradation. This problem might be circumvented using different cation/anion combinations. Compare to silica supports where kinetics are mainly governed by silica/IL interactions, here the release strongly depends on polymer/IL compatibility and polymer degradation.

ACKNOWLEDGMENT

The authors thank Ms Agnès Crepet from the Laboratoire Ingénierie des Polymères UMR 5223 of the University Claude Bernard Lyon 1 for her help with SEC measurements. Mr Didier Cot from the Institut Européen des Membranes of the University of Montpellier is gratefully acknowledged for the SEM images reported here. This work was supported by The Agence Nationale de la Recherche ANR-10-JCJC-0802.

NOTES AND REFERENCES

Electronic Supplementary Information (ESI) available: Figures S1 and S2.

1. J. Bauer, S. Spanton, R. Henry, J. Quick, W. Dziki, W. Porter and J. Morris, *Pharm. Res.*, 2001, **18**, 859-866.
2. W. L. Hough, M. Smiglak, H. Rodriguez, R. P. Swatloski, S. K. Spear, D. T. Daly, J. Pernak, J. E. Grisel, R. D. Carliss, M. D. Soutullo, J. H. Davis and R. D. Rogers, *New J. Chem.*, 2007, **31**, 1429-1436.
3. P. M. Dean, J. Turanjanin, M. Yoshizawa-Fujita, D. R. MacFarlane and J. L. Scott, *Cryst. Growth Des.*, 2009, **9**, 1137-1145.
4. K. Bica and R. D. Rogers, *Chem. Commun.*, 2010, **46**, 1215-1217.
5. K. Bica, J. Shamshina, W. L. Hough, D. R. MacFarlane and R. D. Rogers, *Chem. Commun.*, 2011, **47**, 2267-2269.
6. R. Ferraz, L. C. Branco, C. Prudencio, J. P. Noronha and Z. Petrovski, *ChemMedChem*, 2011, **6**, 975-985.
7. P. D. McCrary, P. A. Beasley, G. Gurau, A. Narita, P. S. Barber, O. A. Cojocar and R. D. Rogers, *New J. Chem.*, 2013, **37**, 2196-2202.
8. H. Mizuuchi, V. Jaitely, S. Murdan and A. T. Florence, *Eur. J. Pharm. Sci.*, 2008, **33**, 326-331.
9. V. Jaitely, A. Karatas and A. T. Florence, *Int. J. Pharm.*, 2008, **354**, 168-173.
10. H. D. Williams, Y. Sahbaz, L. Ford, T.-H. Nguyen, P. J. Scammells and C. J. H. Porter, *Chem. Commun.*, 2014, **50**, 1688-1690.
11. D. Dobler, T. Schmidts, I. Klingenhoefer and F. Runkel, *Int. J. Pharm.*, 2013, **441**, 620-627.
12. M. Moniruzzaman, M. Tamura, Y. Tahara, N. Kamiya and M. Goto, *Int. J. Pharm.*, 2010, **400**, 243-250.
13. M. Moniruzzaman, Y. Tahara, M. Tamura, N. Kamiya and M. Goto, *Chem. Commun.*, 2010, **46**, 1452-1454.
14. C. Ghatak, V. G. Rao, S. Mandal, S. Ghosh and N. Sarkar, *J. Phys. Chem. B*, 2012, **116**, 3369-3379.

15. L. Viau, C. Tourne-Peteilh, J.-M. Devoisselle and A. Vioux, *Chem. Commun.*, 2010, **46**, 228-230.
16. K. Bica, H. Rodriguez, G. Gurau, O. A. Cojocar, A. Riisager, R. Fehrmann and R. D. Rogers, *Chem. Commun.*, 2012, **48**, 5422-5424.
17. T. Ueki and M. Watanabe, *Macromolecules*, 2008, **41**, 3739-3749.
18. J. Le Bideau, L. Viau and A. Vioux, *Chem. Soc. Rev.*, 2011, **40**, 907-925.
19. S. Y. Choi, H. Rodriguez, A. Mirjafari, D. F. Gilpin, S. McGrath, K. R. Malcolm, M. M. Tunney, R. D. Rogers and T. McNally, *Green Chem.*, 2011, **13**, 1527-1535.
20. A. M. A. Dias, S. Marceneiro, M. E. M. Braga, J. F. J. Coelho, A. G. M. Ferreira, P. N. Simoes, H. I. M. Veiga, L. C. Tome, I. M. Marrucho, J. Esperanca, A. A. Matias, C. M. M. Duarte, L. P. N. Rebelo and H. C. de Sousa, *Acta Biomater.*, 2012, **8**, 1366-1379.
21. M. Concepcion Serrano, M. C. Gutierrez, R. Jimenez, M. Luisa Ferrer and F. del Monte, *Chem. Commun.*, 2012, **48**, 579-581.
22. A. M. A. Dias, A. R. Cortez, M. M. Barsan, J. B. Santos, C. M. A. Brett and H. C. de Sousa, *ACS Sustainable Chem. Eng.*, 2013, **1**, 1480-1492.
23. L. X. Bo, B. Wang, Y. Guang and M. Gauthier, *Poly(Lactic Acid)-Based Biomaterials: Synthesis, Modification and Applications, Biomedical Science, Engineering and Technology*, Intech, 2012.
24. R. Auras, L.-T. Lim, S. E. M. Selke and H. Tsuji, *Poly(lactic acid): Synthesis, Structures, Properties, Processing and Applications*, John Wiley & Son, Hoboken, NJ, 2010.
25. K. Park, J. U. Ha and M. Xanthos, *Polym. Eng. Sci.*, 2010, **50**, 1105-1110.
26. H.-Y. Lee, J.-E. Won, U. S. Shin and H.-W. Kim, *Mater. Lett.*, 2011, **65**, 2114-2117.
27. B. Dorj, J.-E. Won, O. Purevdorj, K. D. Patel, J.-H. Kim, E.-J. Lee and H.-W. Kim, *Acta Biomater.*, 2014, **10**, 1238-1250.
28. J. Stoimenovski and D. R. MacFarlane, *Chem. Commun.*, 2011, **47**, 11429-11431.
29. M. L. Focarete, G. Ceccorulli, M. Scandola and M. Kowalczyk, *Macromolecules*, 1998, **31**, 8485-8492.
30. Y. Lin, K. Y. Zhang, Z. M. Dong, L. S. Dong and Y. S. Li, *Macromolecules*, 2007, **40**, 6257-6267.
31. N. Ljungberg and B. Wesslen, *Biomacromolecules*, 2005, **6**, 1789-1796.
32. T. Kawai, N. Rahman, G. Matsuba, K. Nishida, T. Kanaya, M. Nakano, H. Okamoto, J. Kawada, A. Usuki, N. Honma, K. Nakajima and M. Matsuda, *Macromolecules*, 2007, **40**, 9463-9469.
33. J. Zhang, K. Tashiro, H. Tsuji and A. J. Domb, *Macromolecules*, 2008, **41**, 1352-1357.
34. J. M. Zhang, K. Tashiro, A. J. Domb and H. T. Tsuji, *Macromol. Symp.*, 2006, **242**, 274-278.
35. P. J. Pan, B. Zhu, W. H. Kai, T. Dong and Y. Inoue, *Macromolecules*, 2008, **41**, 4296-4304.
36. J. W. Park and S. S. Im, *J. Polym. Sci. Pt. B-Polym. Phys.*, 2002, **40**, 1931-1939.
37. P. J. Pan, J. J. Yang, G. R. Shan, Y. Z. Bao, Z. X. Weng, A. Cao, K. Yazawa and Y. Inoue, *Macromolecules*, 2012, **45**, 189-197.
38. K. I. Park and M. Xanthos, *Polym. Degrad. Stab.*, 2009, **94**, 834-844.
39. *European Pharmacopoeia 7th Edition*, 2013.
40. J. Siepmann and A. Gopferich, *Adv. Drug. Deliv. Rev.*, 2001, **48**, 229-247.